

Knockdown of PKM2 induces apoptosis and autophagy in human A549 alveolar adenocarcinoma cells

BEIBEI CHU^{1,2*}, JIANG WANG^{1,2*}, YUEYING WANG^{1,2} and GUOYU YANG^{1,2}

¹College of Animal Sciences and Veterinary Medicine; ²Key Laboratory of Animal Biochemistry and Nutrition, Ministry of Agriculture, Henan Agricultural University, Zhengzhou, Henan 450002, P.R. China

Received August 6, 2014; Accepted April 30, 2015

DOI: 10.3892/mmr.2015.3943

Abstract. The M2 isoform of pyruvate kinase (PKM2), which has been identified as the predominant cause of the Warburg effect in cancer cells, is essential in tumor metabolism and growth. However, the role of PKM2 in autophagy remains to be elucidated. The present study investigated the effect of PKM2 knockdown on autophagy and apoptotic cell death in human A549 alveolar adenocarcinoma cells. Two short hairpin (sh)RNAs targeting human PKM2 mRNA were designed and lentiviral vectors were constructed. The A549 cells were infected with lentiviruses, containing shRNAs against PKM2, and the expression of PKM2 was examined by reverse transcription-quantitative polymerase chain reaction (RT-qPCR) and immunoblotting analysis. A lactose dehydrogenase (LDH)-coupled enzyme assay was used to detect the pyruvate kinase activity. RT-qPCR was used to detect the mRNA expression level of glycolysis-associated enzymes. The quantification of cells with punctate LC3 and expression of LC3II were examined to demonstrate autophagy. An MTT assay was used to detect cell viability and flow cytometry was used to determine cell apoptosis. The activity of caspase 3/7 and the expression of Bcl-2 were also detected in A549 cells with PKM2 knockdown. The present study demonstrated that the two shRNAs efficiently downregulated the mRNA and protein expression levels of PKM2 in A549 cells. The knockdown of PKM2 decreased pyruvate kinase activity and glycolysis. Autophagy was induced in A549 cells with PKM2 knockdown. Inhibition of autophagy accelerated apoptotic death in PKM2-knockdown cells and this was dependent on

increased caspase 3/7 activity and decreased expression of Bcl-2. In conclusion, the downregulation of PKM2 induced apoptosis and autophagy in A549 cells and this autophagy protected the cells from apoptotic cell death.

Introduction

Autophagy is a self-degradative process whereby organelles and cytoplasm are engulfed, digested and recycled to sustain cell growth (1,2). Autophagy generally supports cancer cell survival in response to metabolic stress; however, unstinted autophagy causes progressive cellular consumption and eventually cell death (3). Autophagy always interplays with apoptosis (4). Several stimuli cause apoptosis and also autophagy in the same cell.

The 'Warburg effect' of cancer cells is predominantly caused by the increased expression of the M2 isoform of pyruvate kinase (PKM2), a rate-limiting enzyme, which catalyzes the conversion of phosphoenolpyruvate (PEP) into pyruvate during glycolysis (5,6). Different from PKL, PKR and PKM1, PKM2 forms not only tetramers (with high affinity for PEP), but also dimers (with low affinity for PEP) (7). The expression levels of PKM2 are increased in diverse types of human cancer and it is hypothesized that PKM2 may be used as a clinical marker of cancer (8,9). Downregulation of PKM2 promotes apoptosis (10,11); however, the role of PKM2 in autophagy remains to be elucidated. The present study investigated the effect of knocking down PKM2 on autophagy and apoptotic cell death in A549 cells.

Materials and methods

Reagents. SYBR Premix Ex Taq, PrimeScript™ RT reagent kit, gDNA Eraser and TRIzol reagent were purchased from Takara Bio Inc. (Otsu, Japan). The 3-(4,5-dimethylthiazol-2-yl)-2,5-diphenyltetrazolium bromide (MTT) reagent, 3-methyladenine (3-MA), pLKO.1 vector, puromycin and mouse anti-human anti-LC3 antibody (1:500; cat. no. L7543) were purchased from Sigma-Aldrich (St. Louis, MO, USA). Chloroquine (CQ) was obtained from InvivoGen (San Diego, CA, USA), and Dulbecco's modified Eagle's medium (DMEM) and fetal bovine serum (FBS) were purchased from Gibco Life Technologies (Carlsbad, CA, USA). Cellulose Nitrate membranes and Luminata™ Crescendo Western Horseradish

Correspondence to: Dr Yueying Wang or Professor Guoyu Yang, College of Animal Sciences and Veterinary Medicine, Henan Agricultural University, 95 Wenhua Road, Zhengzhou, Henan 450002, P.R. China
E-mail: wangyueying2008@126.com
E-mail: haubiochem@163.com

*Contributed equally

Key words: RNA interference, pyruvate kinase M2, apoptosis, autophagy, A549 cells

Peroxidase (HRP) Substrate were purchased from Millipore (Billerica, MA, USA). The protease and phosphatase inhibitors were obtained from Roche (Basel, Switzerland). The rabbit anti-human anti-PKM2 (1:500; cat. no. D78A4), rabbit anti-human anti-cleaved caspase 3 (1:500; cat. no. 5A1E), rabbit anti-human anti-Bcl-2 (1:500; 50E3), rabbit anti-human anti-Bcl-1 (1:1,000; cat. no. D40C5) and rabbit anti-human anti-actin (1:1,000; cat. no. 4967) antibodies were purchased from Cell Signaling Technology, Inc. (Danvers, MA, USA). HRP-conjugated donkey anti-mouse and anti-rabbit immunoglobulin G secondary antibodies were purchased from Jackson Immuno Research Laboratories, Inc. (West Grove, PA, USA). Lipofectamine 2000 and fluorescein isothiocyanate (FITC) Annexin V/Dead Cell Apoptosis kit with FITC-Annexin V and propidium iodide (PI) was purchased from Invitrogen Life Technologies (Carlsbad, CA, USA). Caspase-Glo 3/7 assay was purchased from Promega Corporation (Madison, WI, USA) and a Bicinchoninic Acid (BCA) Protein Assay kit was purchased from DingGuo (Beijing, China).

Establishment of A549 short hairpin (sh)PKM2-1 and A549 shPKM2-2 cells. The A549 cells were grown in monolayers at 37°C in 5% CO₂ and maintained in DMEM, containing 100 units/ml penicillin and 100 µg/ml streptomycin (Sangon, Shanghai, China) sulfate, supplemented with 10% FBS. Two different target sequences for human PKM2 were identified using BLOCK iTTM RNAi designer: shPKM2-1, 5'-GCTGTGGCTCTAGACACTAAA-3' and shPKM2-2, 5'-GTTTCGGAGGTTTGTATGAAATC-3'. These sequences were cloned into the pLKO.1 vector (Sigma-Aldrich). The plasmids, shPKM2-1 and shPKM2-2, were confirmed by DNA sequencing by Sangon. Lentiviral particles were produced by co-transfecting the shPKM2-1 or shPKM2-2 vector with VSVG and D8.9 packaging plasmids (Addgene, Cambridge, MA, USA) into HEK293T cells (American Type Culture Collection, Manassas, VA, USA) using Lipofectamine 2000, according to the manufacturer's instructions. The culture medium, which contained viruses, was collected 48 h post-transfection and used to infect cells. The infected A549 cells were selected in culture medium, containing 4 µg/ml puromycin (Sigma-Aldrich) for 2 weeks.

Immunoblotting. Whole-cell lysates were extracted using radioimmunoprecipitation lysis buffer, containing 50 mM Tris-HCl (pH 8.0), 150 mM NaCl, 1% Triton X-100, 1% sodium deoxycholate, 0.1% SDS and 2 mM MgCl₂, supplemented with protease and phosphatase inhibitors, and the protein concentration was quantified using a BCA Protein Assay kit and a Nanodrop 1000 (Thermo Fisher Scientific, Waltham, MA, USA). The protein samples (10 µg) were separated by 12% SDS-PAGE (Bio-Rad, Hercules, CA, USA) and then transferred onto cellulose nitrate membranes, followed by incubation in 5% non-fat milk for 1 h at room temperature. The membrane was incubated in the primary antibody at 4°C overnight and subsequently incubated in the HRP-conjugated secondary antibody at room temperature for 1 h. The target proteins were detected by using LuminataTM Crescendo Western HRP Substrate and the membranes were exposed to film.

Reverse transcription-quantitative polymerase chain reaction (RT-qPCR). The total RNA was extracted from cells using TRIzol reagent, according to the manufacturer's instructions. Reverse transcription of 1 µg total RNA was performed with the PrimeScriptTM RT reagent kit with gDNA Eraser, according to the manufacturer's instructions. RT-PCR was performed in an Eppendorf Mastercycler[®] ep realplex, according to the manufacturer's instructions. The primers were as follows: Forward: 5'-GCACAGAGCCTCGCCTT-3' and reverse: 5'-CCTTGACATGCCGGAG-3' for β-actin; forward: 5'-GTGCGAGCCTCAAGTCACTCCACA-3' and reverse: 5'-TATAAGAAGCCTCCACGCTGCCCA-3' for PKM2; forward: 5'-GGTGGACCTGGAGAAGCTG-3' and reverse: 5'-GGCACCCACATAAATGCC-3' for PFKL; forward: 5'-GTGCGCATGGGTATCTACG-3' and reverse: 5'-ACTTGCAGGATGCTGGAGAC-3' for PFKP; forward: 5'-GGCTGCGGCTGCTAACT-3' and reverse: 5'-CAGGGCAATGTCAGACAACT-3' for ALDOC; forward: 5'-AGGGGTGTTTTTCCGTAAGC-3' and reverse: 5'-GTTTCAAGCCATTCTGCAT-3' for ACYP1; and forward: 5'-TTGGCTGGGTGAAGAATACC-3' and reverse: 5'-CTAGGGCTTCCAACCTTGCT-3' for ACYP2. β-actin was used as an internal control. The comparative threshold cycle (2^{-ΔΔCT}) method was used to quantify the mRNA expression levels of these genes.

Pyruvate kinase activity assay. A pyruvate kinase activity assay was performed using 2 mg cell lysates in 50 mM Tris-HCl, 100 mM KCl, 5 mM MgCl₂, 1 mM ADP, 0.5 mM PEP, 0.2 mM ADH and 8 units lactate dehydrogenase at 37°C for 30 min. The reduction in absorbance at 340 nm, attributable to the oxidation of NADH, was measured using a microplate reader (Stat Fax-2100; Awareness Technology Inc., Palm City, FL, USA) as the pyruvate kinase activity.

MTT assay. The cells were plated into a 96-well plate at a density of 5x10³ cells/well. The following day, the cells were treated with or without 2 mM 3-MA for 48 h. Medium, supplemented with 0.5 mg/ml MTT was added to the cells. Following culturing for 4 h, the MTT was replaced with 100 µl/well dimethyl sulfoxide. The absorbance at 490 nm was detected using a microplate reader (Awareness Technology Inc.).

Apoptosis analysis. The cells were pretreated with or without 2 mM 3-MA for 48 h and harvested followed by washing in cold phosphate-buffered saline. The washed cells were centrifuged at 1,000 x g and resuspended in 1X Annexin-binding buffer at a final cell density of 1x10⁶ cells/ml. A total of 100 µl of the cells in annexin-binding buffer was obtained and mixed with 5 µl FITC/Annexin V (Component A) and 1 µl of 100 µg/ml PI working solution. Following incubation at room temperature for 15 min, 400 µl of 1X Annexin-binding buffer was added and the samples were maintained on ice. Apoptotic analyses were performed by flow cytometry (BD FACSVerse; BD Biosciences, Bedford, MA, USA), measuring the fluorescence emission at 530 nm and >575 nm. Live cells exhibited only a low level of fluorescence, apoptotic cells exhibited green fluorescence and dead cells exhibited red and green fluorescence.

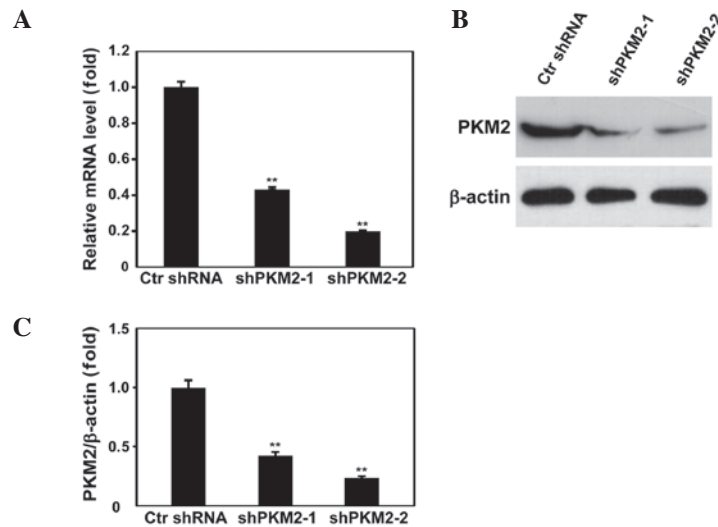


Figure 1. Knockdown of PKM2 in A549 cells. (A) Reverse transcription-quantitative polymerase chain reaction and (B and C) immunoblot analysis of the mRNA and protein expression levels of PKM2, respectively. The results are representative of three independent experiments (** $P < 0.01$, compared with Ctrl shRNA). Ctrl, control; sh, short hairpin.

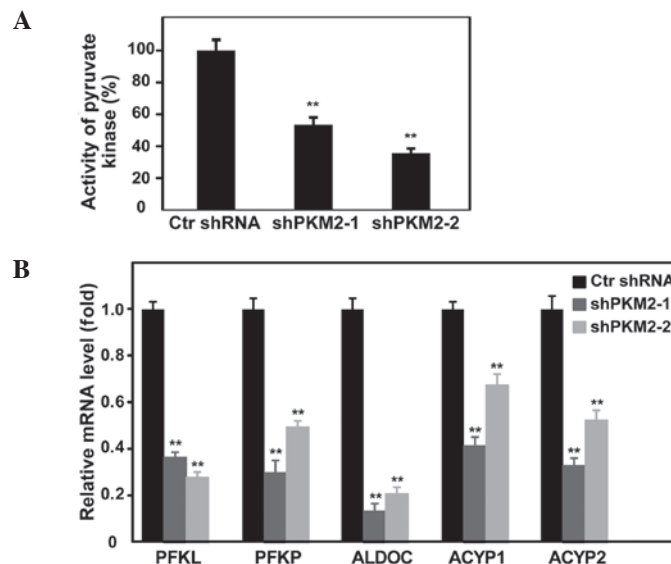


Figure 2. Analysis of the activity of pyruvate kinase and glycolysis. (A) Pyruvate kinase activity was measured with a lactose dehydrogenase-coupled enzyme assay. (B) The mRNA levels of glycolysis-associated genes were detected with reverse transcription-quantitative polymerase chain reaction. The results are representative of three independent experiments (** $P < 0.01$, compared with the Ctrl shRNA). Ctrl, control; sh, short hairpin.

Caspase 3/7 activity assay. The cells were seeded into white-walled 96-well plates to a final cell density at 2×10^3 cells/well and were pretreated with or without 2 mM 3-MA for 48 h. The activity levels of caspases 3/7 were analyzed with the Caspase-Glo 3/7 assay, according to the manufacturer's instructions. Briefly, the plates were equilibrated to room temperature. Caspase-Glo[®] 3/7 reagent (100 μ l) was added into each well. Following incubation at room temperature for 30 min, the luminescent signal was detected with the Fluoroskan Ascent[™] Microplate Fluorometer FL (Thermo Fisher Scientific).

Statistical analysis. The data are expressed as the mean \pm standard deviation. Student's t-tests were performed to determine statistical significance of differences between experimental

groups, using GraphPad Prism 5 (GraphPad Software, Inc., La Jolla, CA, USA). $P < 0.05$ was considered to indicate a statistically significant difference.

Results

Knockdown of PKM2 in A549 cells using two shRNAs. The A549 cells were infected with lentivirus, containing shRNAs against PKM2. The expression levels of PKM2 were analyzed by RT-qPCR and immunoblotting. Each of the shRNAs efficiently decreased the mRNA and protein expression levels of PKM2 in the A549 cells (Fig. 1).

Knockdown of PKM2 decreases the activity of pyruvate kinase and glycolysis in A549 cells. Pyruvate kinase activity was

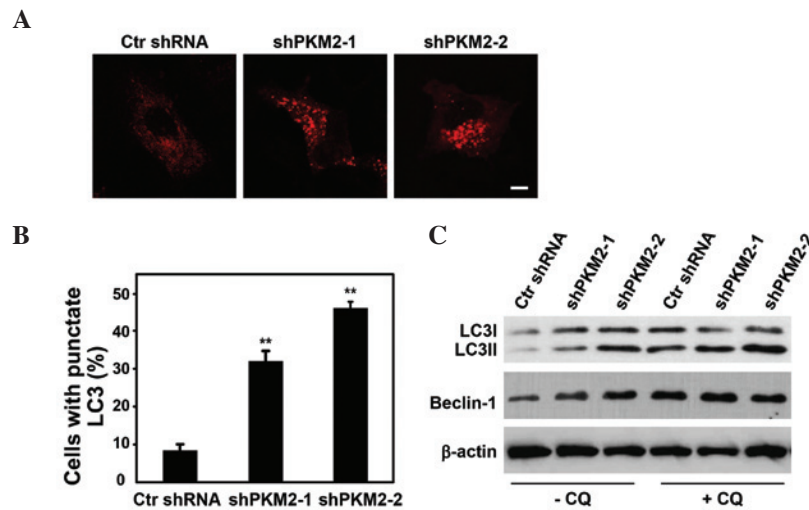


Figure 3. Detection of autophagy. (A) The cells were transfected with mCherry-LC3 and the fluorescence was examined using a confocal microscope (scale bar, 10 μ m). (B) The number of cells with punctate LC3 was quantified and demonstrated as a histogram. (C) Immunoblot analysis was performed using the indicated antibodies. The results are representative of three independent experiments (** $P < 0.01$, compared with the shRNA). Ctrl, control; sh, short hairpin; CQ, chloroquine.

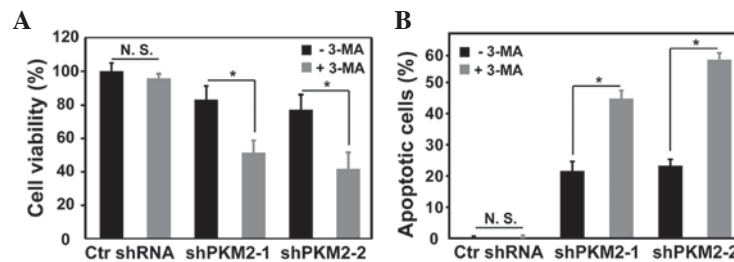


Figure 4. Cell proliferation and apoptotic rates were measured using an 3-(4,5-dimethylthiazol-2-yl)-2,5-diphenyltetrazolium bromide assay and an apoptosis assay. (A) Cell viability was detected using an MTT assay. (B) Annexin V-fluorescein isothiocyanate and propidium iodide staining were performed and flow cytometric analysis was used to detect apoptotic cells. The results are representative of three independent experiments (* $P < 0.05$, compared with the shRNA). Ctrl, control; sh, short hairpin; N.S., not significant; 3-MA, 3-methyladenine.

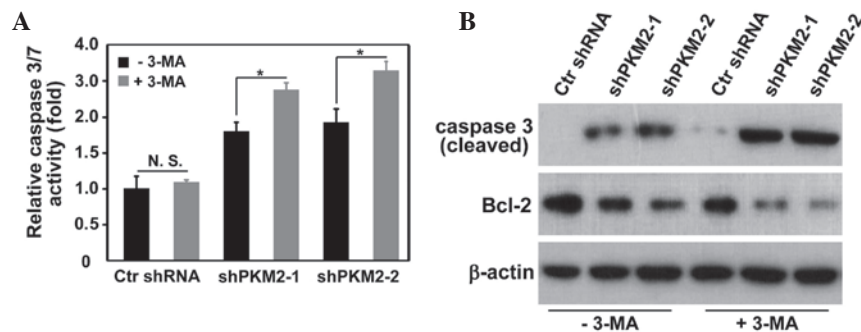


Figure 5. Detection of the activity of caspase 3/7 and the expression levels of Bcl-2. (A) The activities of caspase 3 and 7 were analyzed using the Caspase-Glo 3/7 assay. (B) Immunoblotting analysis was performed with the indicated antibodies. The results are representative of three independent experiments (* $P < 0.05$, compared with the shRNA). Ctrl, control; sh, short hairpin; N.S., not significant; 3-MA, 3-methyladenine.

detected using an LDH-coupled enzyme assay and the mRNA expression levels of glycolysis-associated enzymes were analyzed by RT-qPCR in A549 cells, with or without PKM2 knockdown. Downregulation of PKM2 significantly decreased the activity of pyruvate kinase and glycolysis (Fig. 2).

Knockdown of PKM2 induces autophagy. The quantification of cells with punctate LC3 and the expression levels of LC3II

and Beclin-1 were examined by immunoblotting to assess autophagy in the A549 cells with or without PKM2 knockdown. Downregulation of PKM2 resulted in more cells with punctate LC3, which indicated that autophagy was induced. The expression levels of LC3II and Beclin-1 were upregulated in A549 cells with PKM2 knockdown and use of an autophagy inhibitor, CQ, increased the expression levels of LC3II and Beclin-1 (Fig. 3).

Inhibition of autophagy in A549 cells with PKM2 knockdown promotes apoptotic cell death. Cell viability was detected using an MTT assay and apoptosis was detected using Annexin V/PI staining and flow cytometry in A549 cells with or without PKM2 knock down. Downregulation of PKM2 induced apoptosis and autophagy in the A549 cells. Inhibition of PKM2 induced-autophagy increased apoptotic cell death (Fig. 4).

Inhibition of autophagy in A549 cells with PKM2 knock-down increases the activity of caspase 3/7 and decreases the expression of Bcl-2. Inhibition of autophagy by 3-MA further increased the activity of caspase 3/7 in A549 cells with PKM2 knockdown. Downregulation of PKM2 increased caspase 3 cleavage and decreased the expression of Bcl-2. Inhibition of autophagy using 3-MA caused increased caspase 3 cleavage and markedly lower expression of Bcl-2 (Fig. 5).

Discussion

The metabolic hallmark of cancer cells, unlike normal cells, is aerobic glycolysis (5,6). Increased glucose uptake and increased glycolytic flux occur in cancer cells. The increased conversion of glucose to lactate has been detected in the majority of cancer cells, even under oxygen-sufficient conditions, therefore, facilitating cell proliferation (12). Understanding the molecular mechanisms underlying aerobic glycolysis may assist in controlling carcinogenesis by modulating the metabolic pathways of cancer cells.

PKM2 can be used as a clinical marker of cancer, since it is markedly expressed in cancer cells (8,9). Unlike the other three PKs, PKM2 forms not only tetramers (with high affinity for PEP), but also dimers (with low affinity for PEP) (7). PKM2 is allosterically activated by the glycolytic metabolite fructose-1,6-bisphosphate (13,14). The release of PEP leads to the formation of dimeric PKM2 and a reduction in its catalytic activity, resulting in the accumulation of glycolytic metabolites. These can be used for the synthesis of macromolecular building blocks via the pentose phosphate pathway (15). PKM2 can switch between its dimeric and tetrameric forms in cancer cells (7). If PKM2 forms dimers in cancer cells, the marked expression of PKM2 shifts glucose metabolism to macromolecule biosynthesis to meet the demand of accelerated cancer cell proliferation. The knockdown of PKM2 impaired the mRNA expression levels of glycolytic enzymes (Fig. 2B). AMPK is a master regulator for energy-sensing pathways and is upstream of mTOR (16). The present study hypothesized that the impaired glycolysis in A549 cells with PKM2 knockdown may increase the ratio of AMP/ATP and activate AMPK, therefore, inhibiting mTORC1 kinase activity and promoting autophagy.

Apoptosis and autophagy are pivotal cellular processes, which are important for the maintenance of cell homeostasis. There are several connections between apoptosis and autophagy. One mechanism, which couples apoptosis and autophagy is the interaction of Beclin-1 and Bcl-2 (17). Beclin-1, the mammalian orthologue of yeast Atg6, promotes autophagosomal membrane nucleation (18). The Bcl-2 family performs anti-apoptotic roles in cells (19). Beclin-1 contains a BH3 domain, which is necessary to bind the proteins of

the Bcl-2 family (20-22). The release of Bcl-2 from Beclin-1 activates autophagy (23). The knockdown of PKM2 possibly affects the interaction between Beclin-1 and the Bcl-2 family, which may be caused by reduced expression of Bcl-2. Understanding the intracellular mechanisms, which couple apoptosis and autophagy under the control of PKM2 remain to be elucidated.

In conclusion, to the best of our knowledge, the present study provided the first evidence that downregulation of PKM2 induced apoptosis and autophagy in A549 cells. Pharmacological inhibition of autophagy promoted apoptotic cell death in A549 cells with PKM2 knockdown. These results provided a novel strategy for the treatment of cancer by simultaneously inhibiting PKM2 and autophagy.

Acknowledgements

This study was supported by the China Postdoctoral Science Foundation funded project (no. 124726) and Postdoctoral Sponsorship in Henan Province (no. 2013036).

References

1. Levine B and Klionsky DJ: Development by self-digestion: molecular mechanisms and biological functions of autophagy. *Dev Cell* 6: 463-477, 2004.
2. Mizushima N: Autophagy: process and function. *Genes Dev* 21: 2861-2873, 2007.
3. Baehrecke EH: Autophagy: dual roles in life and death? *Nat Rev Mol Cell Biol* 6: 505-510, 2005.
4. Mariño G, Niso-Santano M, Baehrecke EH and Kroemer G: Self-consumption: the interplay of autophagy and apoptosis. *Nat Rev Mol Cell Biol* 15: 81-94, 2014.
5. Warburg O, Wind F and Negelein E: The metabolism of tumors in the body. *J Gen Physiol* 8: 519-530, 1927.
6. Warburg O: On the origin of cancer cells. *Science* 123: 309-314, 1956.
7. Mazurek S: Pyruvate kinase type M2: a key regulator of the metabolic budget system in tumor cells. *Int J Biochem Cell Biol* 43: 969-980, 2011.
8. Bluemlein K, Gruning NM, Feichtinger RG, Lehrach H, Kofler B and Ralser M: No evidence for a shift in pyruvate kinase PKM1 to PKM2 expression during tumorigenesis. *Oncotarget* 2: 393-400, 2011.
9. Eigenbrodt E, Basenau D, Holthausen S, Mazurek S and Fischer G: Quantification of tumor type M2 pyruvate kinase (Tu M2-PK) in human carcinomas. *Anticancer Res* 17: 3153-3156, 1997.
10. Goldberg MS and Sharp PA: Pyruvate kinase M2-specific siRNA induces apoptosis and tumor regression. *J Exp Med* 209: 217-224, 2012.
11. Spoden GA, Rostek U, Lechner S, Mitterberger M, Mazurek S and Zwierschke W: Pyruvate kinase isoenzyme M2 is a glycolytic sensor differentially regulating cell proliferation, cell size and apoptotic cell death dependent on glucose supply. *Exp Cell Res* 315: 2765-2774, 2009.
12. Mendoza-Juez B, Martínez-González A, Calvo GF and Pérez-García VM: A mathematical model for the glucose-lactate metabolism of in vitro cancer cells. *Bull Math Biol* 74: 1125-1142, 2012.
13. Christofk HR, Vander Heiden MG, Wu N, Asara JM and Cantley LC: Pyruvate kinase M2 is a phosphotyrosine-binding protein. *Nature* 452: 181-186, 2008.
14. Dombrackas JD, Santarsiero BD and Mesecar AD: Structural basis for tumor pyruvate kinase M2 allosteric regulation and catalysis. *Biochemistry* 44: 9417-9429, 2005.
15. Gruning NM, Rinnerthaler M, Bluemlein K, et al: Pyruvate kinase triggers a metabolic feedback loop that controls redox metabolism in respiring cells. *Cell Metab* 14: 415-427, 2011.
16. Hardie DG: AMP-activated protein kinase: a cellular energy sensor with a key role in metabolic disorders and in cancer. *Biochem Soc Trans* 39: 1-13, 2011.

17. Maiuri MC, Ciriollo A and Kroemer G: Crosstalk between apoptosis and autophagy within the Beclin 1 interactome. *EMBO J* 29: 515-516, 2010.
18. He C and Levine B: The Beclin 1 interactome. *Curr Opin Cell Biol* 22: 140-149, 2010.
19. Dietrich JB: Apoptosis and anti-apoptosis genes in the Bcl-2 family. *Arch Physiol Biochem* 105: 125-135, 1997 (In French).
20. Maiuri MC, Zalckvar E, Kimchi A and Kroemer G: Self-eating and self-killing: crosstalk between autophagy and apoptosis. *Nat Rev Mol Cell Biol* 8: 741-752, 2007.
21. Maiuri MC, Le Toumelin G, Ciriollo A, *et al*: Functional and physical interaction between Bcl-X(L) and a BH3-like domain in Beclin-1. *EMBO J* 26: 2527-2539, 2007.
22. Kang R, Zeh HJ, Lotze MT and Tang D: The Beclin 1 network regulates autophagy and apoptosis. *Cell Death Differ* 18: 571-580, 2011.
23. Sinha S, Colbert CL, Becker N, Wei Y and Levine B: Molecular basis of the regulation of Beclin 1-dependent autophagy by the gamma-herpesvirus 68 Bcl-2 homolog M11. *Autophagy* 4: 989-997, 2008.